



HAL
open science

Identification of cellular targets in human intrahepatic cholangiocarcinoma using laser microdissection and accurate mass and time tag proteomics.

Alexandre dos Santos, Magali Court, Valérie Thiers, Sokhavuth Sar, Catherine Guettier, Didier Samuel, Christian Bréchet, Jérôme Garin, France Demaugre, Christophe D. Masselon

► To cite this version:

Alexandre dos Santos, Magali Court, Valérie Thiers, Sokhavuth Sar, Catherine Guettier, et al.. Identification of cellular targets in human intrahepatic cholangiocarcinoma using laser microdissection and accurate mass and time tag proteomics.: Novel cellular targets in human intrahepatic cholangiocarcinoma. *Molecular and Cellular Proteomics*, 2010, 9 (9), pp.1991-2004. 10.1074/mcp.M110.000026 . inserm-00515623

HAL Id: inserm-00515623

<https://inserm.hal.science/inserm-00515623>

Submitted on 31 May 2011

HAL is a multi-disciplinary open access archive for the deposit and dissemination of scientific research documents, whether they are published or not. The documents may come from teaching and research institutions in France or abroad, or from public or private research centers.

L'archive ouverte pluridisciplinaire **HAL**, est destinée au dépôt et à la diffusion de documents scientifiques de niveau recherche, publiés ou non, émanant des établissements d'enseignement et de recherche français ou étrangers, des laboratoires publics ou privés.

Identification of cellular targets in human intrahepatic cholangiocarcinoma using laser microdissection and AMT-tag proteomics.

Alexandre Dos Santos^{1,2}, Magali Court^{3,4,5}, Valérie Thiers^{1,2,6}, Sokhavuth Sar^{1,2}, Catherine Guettier^{1,2,7}, Didier Samuel^{1,2}, Christian Bréchet^{1,2,8}, Jérôme Garin^{3,4,5}, France Demaugre^{1,2}, Christophe D. Masselon^{3,4,5,*}

¹ INSERM, Unité 785, Villejuif, F-94800, France

² Univ Paris-Sud, UMR-S 785, Villejuif, F-94800, France

³ CEA, DSV, iRTSV, Laboratoire d'Etude de la Dynamique des Protéomes, Grenoble, F-38054, France

⁴ INSERM, Unité 880, Grenoble, F-38054, France

⁵ Université Joseph Fourier, Grenoble, F-38054, France

⁶ Institut Pasteur, Département de Virologie, Paris, F-75015, France

⁷ AP-HP Hôpital Bicêtre, Service d'Anatomie Pathologique, Le Kremlin-Bicêtre, F-94270, France

⁸ Merieux Alliance, Lyon, F-69000, France

- **Keywords:** cancer, intrahepatic cholangiocarcinoma, laser microdissection, AMT proteomics, biomarkers

- **Running title:** Novel cellular targets in human intrahepatic cholangiocarcinoma

- **Abbreviations:** AMT, Accurate Mass and Time; CCA, Cholangiocarcinoma; EMT, Epithelial to Mesenchymal Transition; HCC, Hepatocellular Carcinoma; ICC, Intrahepatic Cholangiocarcinoma; LM, Laser Microdissection; TMA, Tissue Micro-Array.

* to whom correspondence should be addressed (email: christophe.masselon@cea.fr)

Abstract

Obtaining accurate protein profiles from homogeneous cell populations in heterogeneous tissues can enhance the capability to discover protein biomarkers. In this context methodologies to access specific cellular population and analyze their proteome with exquisite sensitivity have to be selected. We report here the results of an investigation using a combination of laser microdissection and accurate mass and time tag proteomics. The study was aimed at the precise determination of proteome alterations in intrahepatic cholangiocarcinoma, a markedly heterogeneous tumor. This cancer, which is difficult to diagnose and carries a very poor prognostic, has shown an unexplained increase in incidence over the last few years. Among a pool of 574 identified proteins, we were able to report on altered abundance patterns affecting 39 proteins conforming to a variety of potential tumorigenic pathways. The reliability of the proteomics results was confirmed by Western blot and immunohistochemistry on matched samples. Most of the proteins displaying perturbed abundances had not yet been described in the setting of intrahepatic cholangiocarcinoma. These include proteins involved in cell mobility and actin cytoskeleton remodeling, which may participate in the epithelial to mesenchymal transition, a process invoked in migration and invasion of cancer cells. The biological relevance of these findings was explored using a tissue microarray. An increased abundance of vimentin was thus detected in 70% of intrahepatic cholangiocarcinoma and none of the controls. These results suggest that vimentin could play a role in the aggressiveness of ICC and provide a basis for the serious outcome of this cancer.

Introduction

Cholangiocarcinoma (CCA), which arises from the hepatic bile ducts, is the primary cancer accounting for ~10-15% of all hepatobiliary malignancies. CCA is categorized by the International Classification of Diseases for Oncology into intrahepatic and extrahepatic forms, the latter including perihilar, hilar and distal bile duct CCA. Global incidence rate of intrahepatic cholangiocarcinoma (ICC) has increased by 2-6% during recent decades, while annual incidence rate of the more common, extrahepatic form has remained relatively stable (1, 2). The diagnosis of ICC remains particularly challenging since the disease can mimic metastasis to the liver or hepatocellular carcinoma (HCC). The only potentially curative treatment options available at present are surgical. Unfortunately, the majority of patients are diagnosed at an advanced, unresectable stage because of the initially silent clinical characteristics of this malignancy. The prognosis of ICC is therefore devastating, with survival of less than 24 months following diagnosis. Although several risk factors have been reported as contributing to the development of the disease, most cases of ICC occur in the absence of known etiological factors (3-5). As a consequence, considerable efforts have been made to identify reliable markers to enable the early detection of biliary cancers and provide new insights into the pathogenesis of this deadly disease (6). Recent studies have focused on the cytokines and growth factors (7, 8) produced by CCA cells, as well as on the proteomic analysis of serum and bile (9, 10). Follow-up studies are ongoing to determine the sensitivity and specificity of the markers that have emerged from these investigations.

Tumor tissue is undeniably the most appropriate resource to investigate tumor-specific signals. Indeed, the determination of alterations to the protein profiles of ICC may offer opportunities to identify tumor-specific markers. To date, proteomics studies performed using tumor tissues have mainly tried to identify proteins with a differential expression between HCC and ICC in order to prevent the misclassification of these pathologies (11, 12). Furthermore, these studies, performed on total liver homogenates, were not appropriate to detect proteins with altered expression in tumorous

cholangiocytes. Indeed, ICC tumor cells are essentially embedded in an abundant stroma containing inflammatory cells and fibroblasts, which may impair the detection of proteins displaying tumor-specific expression patterns (13). In summary, because no proteomics studies have so far been performed on isolated cholangiocytes, any proteome alterations in the setting of ICC remain a matter of speculation.

Laser microdissection (LM) has emerged as a suitable tool to selectively extract cells of interest from their natural environment. This technology has been employed extensively to profile global gene expression in purified tumor cells (14-16). It has also been used successfully in experiments designed to discover protein biomarkers through mass spectrometry-based proteomics studies (17-19). However, working with such small samples challenges conventional proteomics techniques in terms of sensitivity and the precision of quantitation.

One particularly efficient method for proteome analysis is the so-called Accurate Mass and Time (AMT) tag approach, where high performance liquid chromatography (HPLC) and high resolution Fourier transform ion cyclotron resonance mass spectrometry (FTICR-MS or FTMS) work in synergy to achieve a broad proteome coverage, even for small sample amounts (20, 21). A recent report demonstrated the significant advantage of the AMT tag method over more conventional proteomics technologies in enabling significantly broader proteome coverage using the minute protein quantities available from tissue microdissection (22).

In the present study, we used an AMT tag strategy to determine the differential protein profile between tumorous and non tumorous microdissected cholangiocytes, in order to define specific proteome alterations of human ICC. Among proteins with altered expression in ICC, we detected a panel of proteins conforming to potential tumorigenic pathways which could be candidates as therapeutic targets and tumor markers for this lethal disease.

Experimental Procedures

- Patients and tissue samples

Liver specimens were obtained from the “Centre de Ressources Biologiques Paris-Sud”, Paris-Sud University, France. Access to this material was in agreement with French legislation. Tissue samples were collected at the time of surgical resection with the prior informed consent of patients. The local research ethics committee specifically approved this procedure. Detailed clinical data regarding these subjects are summarized in Table 1. Tumorous and adjacent non-tumorous hepatic tissues from four patients with intrahepatic cholangiocarcinoma and five perihilar samples containing large bile duct sections from control subjects without ICC, were obtained within 30 minutes of surgical resection. These samples were immediately frozen in liquid nitrogen and stored at -80°C until use. The tumors were graded by a pathologist by means of microscopic examination.

- Laser microdissection (LM)

The liver sections were prepared and treated as previously described (23). LM was performed using a PALM Microbeam system (Carl Zeiss Inc.) (see Supplementary Figure 1). From each liver sample, approximately 100,000 cells corresponding to 10 mm^2 were microdissected and catapulted directly into the cap of a microcentrifuge tube containing $10\mu\text{l}$ 10% SDS. Cell lysates were stored at -80°C until use. Based on a careful review, each section was estimated to contain $\geq 90\%$ of the desired cells.

-Mass spectrometry analysis

1- Sample preparation

For AMT tag database generation, LC-MS/MS analyses have to be performed on fractionated samples to achieve decent proteome coverage. For this purpose, four to six samples were pooled per pair of patients with or without ICC (Figure 1A). Thirty microliters of lysis buffer (50mM Tris pH 6.8, 2% SDS, 0.35M beta-Mercaptoethanol and 4M urea) were added to each pool and the samples

were deposited on a 1D-SDS-PAGE gel before being subjected to a short separation (pseudo-stacking) in order to prevent the sample from being distributed over the whole gel lane. After Coomassie Blue staining to reveal proteins, each pseudo-stacking band was cut into 8 slices and the corresponding fractions were digested in-gel with trypsin (Promega, Charbonnières-les-bains, France), as described previously (24). An estimated 0.8 to 1.2 μg of total protein was injected for each gel fraction. All fractions were analyzed with LC-MS/MS in triplicate and the resulting peptide identifications were used to compile an AMT tag database.

For quantitative studies, protein extracts from individual patient biopsies were deposited on 1D-SDS-PAGE gel and migrated in the stacking mode (Figure 1B). The stacked gel band associated with each patient was then excised and digested in-gel as described above. The resulting peptide mixtures were analyzed in triplicate using LC-FTMS. Peptides from approximately 20,000 cells were injected for each LC-FTMS analysis.

2- nano-HPLC-MS and MS/MS analysis

All proteomic analyses were performed using the 7-tesla hybrid linear ion trap Fourier transform ion cyclotron resonance mass spectrometer LTQ-FT Ultra (Thermo Electron, Bremen, Germany) coupled to an Ultimate 3000 (LC-Packings, Amsterdam, Netherlands) nano HPLC system mounted with an LC-Packings Pepmap nano-column (75 μm ID, 15 cm long, 3 μm particles, 100 \AA pores). The chromatographic separation conditions were as described previously (25).

2.1- AMT tag database generation (MS/MS mode)

The FTMS detector was used for the survey scan within the m/z range of 400-1850 at a resolution setting of 50,000 (25). MS/MS was performed in the linear ion trap in parallel with high resolution acquisition of the MS signal on the FT detector. Dynamic exclusion prevented the acquisition of multiple MS/MS spectra for a given precursor ion (mass tolerance = ± 2 ppm, repeat MS/MS acquisition = 2x within 30 s, exclusion duration = 180 s, exclusion list size = 500 entries.)

MS/MS data were processed using Mascot Distiller (Matrix Science, UK) to produce peak lists (e.g. .mgf files) that were subsequently submitted to the Mascot v.2.2.03 (Matrix Science, UK) search engine for database searches against the SwissProt-TREMBL database (compiled from SwissProt release v54.8 and TREMBL release v37.8) using the taxonomy “Homo sapiens (human)” (72,036 protein sequences). Mascot search parameters are listed in supplementary Table 1. A target-decoy database search was performed as described previously (26) in order to estimate false positive rates. Identifications were validated automatically (Filters: Rank=1 + score>identity threshold at p-value<0.05) and compiled in an MS identification database using the IRMa home-made software (27). The MS identification database was then converted into an AMT tag database (Microsoft Access format) by grouping the multiple occurrences of each identified peptide. To reduce false positives, we opted for the removal of peptides with length ≤ 6 amino acids. In addition, only proteins covered by at least two peptides were considered for inclusion in the database, with the exception of proteins covered by a single peptide (length >6) with a Mascot score greater than or equal to 50. Peptides spectrum matches for these peptides have been compiled and are provided as supplementary figure 2.

2.2- Quantitative MS acquisitions (MS mode)

All quantitative MS data were obtained under the FTMS detection mode on an m/z range of 400-1850 and resolution of 50,000. We took advantage of the parallel acquisition capability of the LTQ-FT instrument to acquire a single MS/MS spectrum during each survey scan. This allowed us to further populate the AMT tag database without compromising the MS data acquisition rate.

MS data were processed using the Decon-2LS/VIPER open-source software suite provided by PNNL (see <http://ncrr.pnl.gov/>). Individual MS spectra were de-isotoped using Decon-2LS. The VIPER software then ensured LC-MS feature detection, retention time alignment and feature identification in the AMT tag database, as previously described (28) We opted to further filter the

list of identifications by keeping only matches with a confidence score (i.e. SLIC score)(29) higher than 0.9.

2.3- Statistical analysis

In order to extract lists of peptides that were differentially abundant in the two cholangiocytes populations, we applied a statistical analysis to the data based on the Spectral Index (SpI) approach proposed by Heineke and coworkers (30). The SpI method was developed in the context of label-free quantification using spectral counting techniques (31). It was necessary to adapt it slightly to fit the needs of our AMT-based label-free strategy which is reliant on peptide signal extraction. To achieve this, we replaced protein spectral counts by individual peptide abundances, and instead of defining the SpI for each identified protein, we defined an Abundance Index (AbI) for each identified peptide. The AbI was thus defined as:

$$AbI = \left(\frac{\bar{A}}{\bar{A} + \bar{B}} \times \frac{N_A^D}{N_A^T} \right) - \left(\frac{\bar{B}}{\bar{A} + \bar{B}} \times \frac{N_B^D}{N_B^T} \right) \quad (1)$$

Where \bar{A} (resp. \bar{B}) was the average abundance of a peptide in the population A (resp. B); N_A^D and N_B^D the numbers of patients in each population where the peptide was detected; and N_A^T and N_B^T the total numbers of samples in each population. The distribution of observed AbI for all the detected peptides was then compared to the AbI distribution obtained by random permutation of the datasets across the two populations in order to estimate the variance. Permutations thus allowed the establishment of a confidence interval to assess differential abundances. It is worth mentioning here that, although the AbI method was designed to handle missing values, it is only applicable to peptides which have been detected at least once in each population. All calculations were performed using JMP v.7.0.1 software (SAS institute Inc.).

3- Immunochemical analysis

3.1- Western blot analysis.

For Western blot analysis, samples from the batches of microdissected cholangiocytes were run on SDS-PAGE and transferred onto nitrocellulose membranes as previously described (23). The membranes were then blocked with PBS/ 5% skimmed milk / 0.1% Tween 20 for two hours at room temperature before being incubated overnight with appropriate dilutions of antibodies raised against Vimentin (DAKO, V9 clone), carbonic anhydrase II (Santa Cruz Biotechnology) and profilin-1 (Cell Signaling Technology). The primary antibody was detected using appropriate horseradish peroxidase-coupled secondary antibodies and the ECL plus kit (GE Healthcare) for signal visualization.

3.2- Construction of tissue microarray

The hepatic tumors selected for inclusion in a tissue microarray (TMA) comprised 23 ICC, 17 hilar cholangiocarcinoma, 19 HCC and 22 non-tumorous liver samples (see supplementary Table 2). All cases were reviewed by a pathologist. Intrahepatic cholangiocarcinoma cases were categorized as trabeculo-tubular (19 cases) or invasive papillary (4 cases) carcinomas. Before arraying, sections from each tissue block were stained with hematoxylin and eosin in order to define morphologically representative areas of the tumor. Three tissue cylinders with a diameter of 1 mm were then punched from carefully selected, morphologically representative regions of each donor tissue block and deposited in a recipient block using a tissue-arrayer (MTAI Beecher Instruments). Four micrometer thick sections of this array block were stained with hematoxylin and eosin to enable histological verification of the adequacy of the arrayed tumor tissues.

3.3- Immunohistochemical analysis

Immunohistochemical analysis was performed using formalin-fixed and paraffin-embedded tissue specimens that were matched with the samples used for LM. Deparaffinized 4-micrometer thick sections were treated with primary antibodies against vimentin and carbonic anhydrase II overnight at 4°C after appropriate antigen retrieval treatment. Primary antibody/antigen binding was detected using the Vectastain ABC system (Vector Laboratories). Nuclei were counterstained with

hematoxylin. Labeling specificity was determined by omitting the primary antibody during the experiment. Using the same procedure, labeling of microarrayed tissue sections by the anti-vimentin antibody was carefully analyzed by a pathologist, and was considered to be negative when fewer than 5% of the cells of interest were immunostained. Statistical significance was calculated using a two-tailed Fisher's exact test under StatEl software (www.adscience.eu), with $p < 0.01$ for statistical significance.

Results

A major feature of ICC is the presence of an important stromal reaction in the tumor. Thus in order to obtain protein abundance profiles that were relevant to ICC tumor cells, we opted for the laser microdissection technique so as to collect enriched populations of cholangiocytes (see supplementary Figure 1). ICC tumor cells were isolated from the livers of four patients. Biliary cells dissected from large bile ducts present in the perihilar sections of the livers of five patients without ICC or any biliary tract pathology were used as controls.

Proteomics study using an AMT tag strategy

Generation of an AMT tag database

The first step in the AMT tag methodology consists in generating a database of peptides that can be identified in the sample under study. To achieve this, we analyzed peptide mixtures resulting from digestion of the various fractions obtained from pools of microdissected cells separated on 1D gels (see Figure 1A). Following LC-MS/MS analysis and Mascot search, peptide identifications were compiled in a so-called AMT tag database. Only proteins identified by at least two peptides were considered for inclusion, except when a single peptide had a Mascot score higher than 50. In total, 21,902 peptide identifications were validated and grouped by sequence, molecular weight and average retention time. The median Mascot score for the peptides that passed our filtering criteria for inclusion in the AMT database was 50.56, and 90% of the peptides considered scored higher than 33.27. The resulting AMT tag database thus contained 2,499 distinct peptides indicative of

4,508 protein accessions. When shotgun approaches are used for protein identification, a certain degree of redundancy can be observed in the list of proteins identified. Indeed, several proteins in our database, and particularly isoforms or sequence variants, were covered by the same sub-sets of peptides. In order to reduce this redundancy in the protein list, proteins characterized by the same sub-set of peptides were grouped into so-called protein groups (32). Supplementary Table 3 lists the 574 protein groups thus identified, and the individual proteins within these groups. This list can be considered as the minimal list of proteins required to account for all the peptides identified. In fact, the average peptide coverage for the 574 proteins incorporated in the AMT database was of the order of five peptides per protein.

The sub-cellular localization of identified proteins was determined using Ingenuity Pathway Analysis software (<http://www.ingenuity.com>). As shown in supplementary figure 3, while the majority (67.4%) of the proteins identified were from the cytoplasm, notable proportions (18.4% and 6.5%) arose from the nucleus and plasma membrane respectively. Overall, most sub-cellular compartments were represented in the AMT database, suggesting that our approach enabled access to a broad cross-section of cellular proteins.

Label-free quantitative LC-FTMS data evaluation

After compiling the AMT tag database, we then considered the quantitative data obtained by LC-FTMS analysis of individual microdissected samples (see Figure 1B). Following data acquisition, several tests were performed to assess their quality. This was achieved by evaluating the raw signals in all analyses using dedicated software, and by calculating correlations between the peptide abundances obtained by different acquisitions. The Chaorder software (33) was used as a first means of data evaluation. This algorithm based on a score that measures the similarity between pairs of mass spectra enables an assessment of reproducibility and similarity between LC-MS experiments. For this purpose, Chaorder computes a pseudo-distance between acquisitions based solely on the raw signal. According to Prakash et al. (33), a distance between two points between 0

and 0.2 represents levels of reproducibility usually seen in repeat experiments with the exact same experimental setup. Figure 2A shows the Chaorder plot obtained by comparing the LC-MS acquisitions collected during our experiment. Given the randomized order in which analyses were performed, the limited scattering of replicate acquisitions of the same sample was indicative of an absence of significant drift in the analytical system. Data consistency was further evaluated using pairwise correlations of peptide abundances between acquisitions. The higher the Pearson coefficient, the more alike the two datasets were. When plotting the correlation matrix of all experiments (see Figure 2B), it became clear that triplicate experiments on the same subject always resulted in strongly correlated abundances ($R = 0.94 \pm 0.04$).

Determination of deregulated proteins

Before statistical analysis, triplicate acquisitions of the same sample were combined by averaging the abundances in all runs for each peptide that had been detected at least in two of the three replicates. This procedure produced four cancer and five control datasets (see supplementary Table 4). During the quantitative study, we were able to detect and quantify approximately 1850 of the 2,499 previously sequenced peptides corresponding to 349 proteins identified by at least two peptides.

The nine datasets were subjected to statistical analysis, based on the approach proposed by Heineke and coworkers (30). This method combined the relative species abundance and the number of cases within a group for which the species was detected into a so-called “Abundance index” (AbI). Permutation analysis then enabled the establishment of a confidence interval to assess differential abundances. The resulting distributions of AbI obtained for all the detected peptides in the two populations are shown in Figure 3. Peptides with AbI values falling outside the 95% confidence interval [$-0.25 < \text{AbI} < 0.53$], based on permuted data, were determined to be differentially abundant between tumorous and control cholangiocytes ($p < 0.05$). Peptides were then grouped into proteins, and only proteins for which at least one proteotypic peptide was detected with differential

abundance between the two cholangiocyte populations were retained. This process led to a list of 82 peptides (associated with 23 proteins) with decreased abundance in tumorous cholangiocytes and 42 peptides (corresponding to 16 proteins) with higher abundance in these cells (see Table 2).

With respect to functional considerations, most proteins identified with an altered expression in tumorous cells could be grouped in two categories: A first pool of proteins was associated with metabolic pathways (glycolysis, neoglucogenesis or fatty acid metabolism), and a second consisted of proteins involved in cell structure and/or motility.

It is worth noting that only peptides detected at least once in each population (ICC and controls) are amenable to this type of statistical analysis. As a matter of fact, several peptides were detected only in one of the two populations. When assigning these peptides to proteins, it turned out that several proteins exclusively covered by population-specific peptides were involved in biological process relevant to carcinogenesis (see supplementary Table 5). Among them, the up-regulation of Mac 2 binding protein (LGALS3BP), a metastasis relative protein C (34), had been reported in various cancers including biliary tract carcinoma (35). Likewise, IQGAP2 had shown reduced levels in cancers, and the targeted disruption of the murine IQGAP2 gene resulted in the development of HCC (36, 37).

Confirmation of proteomics findings

Western blot and immunohistochemistry on matched samples.

In order to verify the reliability of the data obtained during this study, the expression of vimentin, profilin1 and carbonic anhydrase II (CAII) was assessed using Western blot in microdissected cholangiocytes from the patients and controls included in the proteomic analysis. As determined during mass spectrometry analysis (Figure 4A), the expression of vimentin and profilin1 was stronger in ICC samples, whereas the immunolabeling of CAII was reduced in these samples when compared with the controls (Figure 4B).

These results were further corroborated when altered abundance patterns for vimentin and CAII were detected in cholangiocytes using immunohistochemistry (Figure 4C). Tissue sections from formalin-fixed and paraffin-embedded tissue specimens matched with the samples used for the microdissection of cholangiocytes were covered by this analysis. CAII was only detected in biliary ducts from control livers and non-tumorous areas of the ICC, whereas anti-CAII antibody did not label tumorous cholangiocytes. Conversely, the anti-vimentin antibody labelled vascular smooth muscle, Kupffer and inflammatory cells in the analyzed tissue sections. However, vimentin was not detected in cholangiocytes lining normal biliary ducts from the control liver or non-tumorous area of the cholangiocarcinoma, but was revealed in tumorous intrahepatic cholangiocytes. Similar results were obtained with the other tissue specimens (data not shown). Taken together, these data established the reliability of our data and the robustness of our strategy regarding the identification of proteins displaying altered expression in the setting of ICC.

Vimentin expression in primary liver cancers.

In order to further validate the over-abundance of vimentin in ICC, the expression of this protein was examined using a tissue microarray comprising samples from a series of patients with primary liver cancers including ICC, hilar CCA and HCC. Briefly, we confirmed, in a larger series of liver samples, that vimentin was not detected in non-tumorous cholangiocytes (0/22) but was expressed in the tumor cells of most (16/23) ICC samples included in the tissue microarray. On the other hand, only 2/17 hilar CCA and 1/18 HCC showed positive staining for vimentin in tumor cells. The specificity of vimentin expression in ICC was established by statistical analysis using Fisher's test (see Figure 5).

Discussion

To our knowledge, this is the first study to investigate the proteome alterations that occur in ICC while taking account of the important cellular heterogeneity of this tumor. Our strategy combining LM to select cholangiocytes, and an AMT tag proteomics methodology appropriate for the analysis of small cellular samples, was devised to overcome this challenge. And indeed, this strategy provided strong evidence of specific alterations to glycolysis and organization of the cytoskeleton, two protein networks involved in carcinogenesis.

ICC is a devastating cancer with an incidence increasing worldwide. For this reason, studies have been carried out in recent years to clarify the mechanisms underlying the development of this cancer, with the aim of developing novel therapeutic strategies. These investigations provided evidences that ICC was associated with genetic alterations (38-40) and impaired protein expression that could contribute to the proliferation of tumorous cholangiocytes (41, 42). Until now, global genome and proteome alterations in ICC have been the subject of little investigation. In particular, proteome impairments in ICC had only been explored during one study using liver homogenates (43). Indeed, the accurate determination of proteome alterations in ICC is a particularly challenging task, because in most tumors, cholangiocytes are embedded in an abundant stroma that may mask cholangiocyte signals. Therefore, in order to obtain accurate insights into proteome alterations in ICC, we used LM to selectively extract cholangiocytes from liver specimens.

Another important prerequisite to this study was the choice of a proteomics technique appropriate for the analysis of small samples. An AMT tag strategy was adopted because this method had been shown to significantly improve proteome coverage for samples originating from microdissected breast carcinoma cells (22). In order to exploit each specimen to the maximum, we used microdissected cholangiocytes both for the generation of the AMT tag database and the quantitative study. The resulting AMT database contained 2,499 distinct peptides belonging to 574 proteins, 460 of these being characterized by at least two peptides.

The first step in quantitative data processing consisted in assessing data quality using two independent methods: Chaorder and pairwise correlations. As can be seen from the Chaorder plot (Figure 2A), and the pairwise correlation matrix (Figure 2B), acquisitions corresponding to the same patient displayed less dispersion, respectively better correlations, than analyses of unrelated samples, even though the run order was randomized. Moreover, acquisitions corresponding to the controls tended to display better homogeneity than those of cancer patients. The Chaorder plot and the correlations between replicates thus confirmed that our data were consistent with samples classification and that no outlier run was present.

We then proceeded to extract the list of peptides that were differentially abundant between the two populations using an abundance index (AbI) methodology. The observed AbI distribution was skewed toward positive values (see Figure 3A), suggesting that the abundance of peptides in tumorous samples was slightly higher than in the control samples. Taking account of this observation, we therefore considered the median AbI value (0.140) as the reference point at which there was no difference between cancer and control samples. Statistical processing and the subsequent filtering of proteins for which no proteotypic peptides were found to be deregulated led to a list of 23 proteins with decreased abundance in ICC and 16 proteins exhibiting higher abundance in tumor cells (see Table 2). We believe that the rigorous criteria chosen to perform this proteomic study warrant a high level of confidence in the final list of deregulated proteins. Indeed, using alternative methods (Western-blot and immunohistochemistry), the altered expression of some of them (vimentin, profilin 1 and CAII) could be confirmed in tumorous cholangiocytes (see Figure 4).

Many of the altered proteins in tumorous cholangiocytes were involved in glycolysis and regulation of the cytoskeleton. As previously observed in kidney and pancreatic cancers (44, 45), we detected an increased abundance of proteins from the glycolytic pathway in ICC. In addition to M2-PK, we were able to identify fructose biphosphate aldolase A and lacticodehydrogenase A. These findings

indicate, as suggested many years ago by Otto Warburg (46) for other tumor cells, that glycolysis could also be altered in tumorous cholangiocytes. It has recently been shown that aerobic glycolysis, a distinctive feature of tumor cells, requires the overexpression of M2-PK, and provides a selective growth advantage for these cells (47). We therefore hypothesize that an overabundance of this isoform may participate in the development of ICC.

We also noted an altered protein network involved in cytoskeleton organization and cell motility. In particular, we noticed a striking increase in the abundance of vimentin, an intermediate filament protein. This protein, expressed in a number carcinomas, has been shown to correlate with the invasiveness and poor prognosis of these tumors (48-52). We also demonstrated the impaired expression of a group of proteins implicated in the equilibrium between globular and filamentous actin. This process, altered during cell transformation (53, 54), is involved in cell motility, which is notably increased during invasion and metastasis (55, 56). We found an increase in the abundance of actin-binding proteins (Cofilin1, Profilin1, Transgelin2). Cofilin1 had been reported as being over-expressed in gastrointestinal endocrine tumors, and the aggressiveness of these tumors had been linked with the expression of this protein (57). As for Profilin1 and transgelin2, a contrasting expression pattern had been reported in breast and colon cancers (58, 59). The functional significance of these differences needs to be clarified, particularly since these proteins had been described as tumor suppressors (60, 61).

We also observed an over-abundance in ICC of S100A11 (Calgizzarin), a protein involved in the Ca^{++} signaling network and in the regulation of cell growth and motility (62, 63). Such alterations had also been reported in pancreatic (64) and colon cancers, where disease progression correlated with the abundance of this protein in tumor tissues.(65, 66).

On the other hand, annexins exhibited lower abundance in our ICC samples compared to the controls. Increased expression of annexins had been reported in different types of carcinoma, e.g. colorectal, bladder, pancreatic, hepatocellular and renal carcinomas (67-71). However, a reduced

expression of annexin A2, also observed in head and neck squamous cell and prostate carcinomas (72, 73) and osteosarcoma (74), had been linked to the aggressive behavior and metastatic potential of these tumors.

Similarly, as reported in renal carcinoma (75), we observed that the catalytic subunit alpha 1 of Na/K ATPase was under-represented in ICC samples. Na/K ATPase had been reported as regulating carcinoma cell motility (76) and had been shown to be involved in tight junction formation during the biogenesis of polarized cells (77). It has thus been speculated (75) that reduced Na/K ATPase activity might be implicated in the loss of cell-cell adhesion.

Cancer cells attain the migratory and invasive capacities required for metastasis by undergoing a phenotypic conversion referred to as the Epithelial to Mesenchymal Transition (EMT) (78). The expression of TGFbeta, a potent inducer of EMT (79) is increased in many human cancers (80) including ICC (81, 82). Interestingly, the protein alterations found in tumorous cholangiocytes (present study) displayed striking similarities with those reported in A549 human lung adenocarcinoma cell line (83) during TGFbeta-induced EMT. Specifically, similar impairments of vimentin, M2-PK, cofilin1, transgelin 2, Na/K ATPase and S100A11 expression were observed in both cases, suggesting that the protein profile of tumorous cholangiocytes fits with that of epithelial cells displaying a transition to the mesenchymal phenotype.

Vimentin is a mesenchymal marker that had been reported to be over-expressed in a number of cancers, its expression being associated with EMT (78). During the present study, we were able to confirm using tissue microarrays that the over-expression of vimentin was a typical feature of ICC because 16 out of 23 (~70%) of the tumors studied expressed this protein. Further experiments will be necessary to correlate this finding with EMT. If confirmed, however, this hypothesis might provide a basis for the serious outcome of this cancer. It is worth noting that all invasive papillary tumors included in the TMA were negative for vimentin (see supplementary table 2 and supplementary figure 4), suggesting that these tumors could represent a subtype of ICC. Studies on

a larger patient population (with trabecular and papillary cases) are underway to assess the generality of these findings. Interestingly, an increased abundance of vimentin was not found in all types of CCA: it was only detected in two out of the 17 tumors analyzed from patients with hilar CCA. As previously shown by Guedj *et al.* (84), this tends to confirm that hilar CCA and ICC are distinct entities displaying specific protein abundance profiles. Similarly, vimentin expression was not found to be a common feature in HCC: it was only expressed in one out of the 18 tumor tissue samples analyzed. Overall, these findings suggest, as reported in others cancers (44-48), that vimentin could play a role in aggressiveness of ICC and provide a basis for the serious outcome of this cancer.

Conclusion

Until now, owing to the important cellular heterogeneity of ICC, the specific protein profile of these tumors could not be adequately determined. In the present study, we selected an appropriate strategy based on LM and AMT tag proteomics, in order to access specific cellular populations and analyze their proteome with high sensitivity. We were thus able to describe a panel of 39 proteins showing altered abundance profiles in tumorous *vs.* healthy cholangiocytes. Most of the proteins displaying perturbed abundances had not yet been described in the setting of ICC. Interestingly, a majority of deregulated proteins were involved in glycolysis and cytoskeleton plasticity/cell motility, pathways that had been reported to be implicated in carcinogenesis. While further experiments are required to characterize the consequences of these deregulations, we anticipate that these data may open the way to novel therapeutic targets or diagnostic tools. In particular, achieving a specific diagnosis of ICC among other primary liver cancers is often problematic. Results from our tissue microarray experiment suggest that vimentin, in combination with other markers, might prove useful as an indicator of particular subtypes of ICC. This will be the subject of a follow-up study on a larger number of patients with ICC, hilar CCA and HCC.

Acknowledgements:

This work was supported by the Institut National du Cancer (grant PL027). A Marie Curie international reintegration grant to C.D.M (contract MIRG-CT-2006-30810) is gratefully acknowledged. A.D.S was supported by a fellowship from the Institut National du Cancer (grant PL027). The authors gratefully acknowledge Pr Valerie Paradis for tissue procurement. We would like to thank Christophe Bruley and Véronique Dupierris for their assistance with setting up the AMT tag database, Sabine Brugière for her assistance with the analytical setup, and Virginie Hossard for TMA construction. Laser microdissection was performed with technical assistance from Sylvie Dumont at the Laser microdissection core facility directed by Dominique Wendum at IFR65, Saint Antoine, Paris, France. The Decon-2LS and VIPER software used for data processing were provided by the W.R. Wiley Environmental Molecular Science Laboratory, a national scientific user facility sponsored by the U.S. Department of Energy's Office of Biological and Environmental Research, located at PNNL. PNNL is operated by Battelle Memorial Institute for the U.S. Department of Energy under contract DE-AC05-76RL0 1830.

References:

1. Patel, T. (2001) Increasing incidence and mortality of primary intrahepatic cholangiocarcinoma in the United States. *Hepatology* **33**, 1353-1357.
2. Ustundag, Y., and Bayraktar, Y. (2008) Cholangiocarcinoma: a compact review of the literature. *World J Gastroenterol* **14**, 6458-6466.
3. Ben-Menachem, T. (2007) Risk factors for cholangiocarcinoma. *Eur J Gastroenterol Hepatol* **19**, 615-617.
4. Blechacz, B. R., and Gores, G. J. (2008) Cholangiocarcinoma. *Clin Liver Dis* **12**, 131-150, ix.
5. El-Serag, H. B., Engels, E. A., Landgren, O., Chiao, E., Henderson, L., Amaratunge, H. C., and Giordano, T. P. (2009) Risk of hepatobiliary and pancreatic cancers after hepatitis C virus infection: A population-based study of U.S. veterans. *Hepatology* **49**, 116-123.
6. Bonney, G. K., Craven, R. A., Prasad, R., Melcher, A. F., Selby, P. J., and Banks, R. E. (2008) Circulating markers of biliary malignancy: opportunities in proteomics? *Lancet Oncol* **9**, 149-158.
7. Alpini, G., Invernizzi, P., Gaudio, E., Venter, J., Kopriva, S., Bernuzzi, F., Onori, P., Franchitto, A., Coufal, M., Frampton, G., Alvaro, D., Lee, S. P., Marzioni, M., Benedetti, A., and DeMorrow, S. (2008) Serotonin metabolism is dysregulated in cholangiocarcinoma, which has implications for tumor growth. *Cancer Res* **68**, 9184-9193.
8. Ohira, S., Itatsu, K., Sasaki, M., Harada, K., Sato, Y., Zen, Y., Ishikawa, A., Oda, K., Nagasaka, T., Nimura, Y., and Nakanuma, Y. (2006) Local balance of transforming growth factor-beta1 secreted from cholangiocarcinoma cells and stromal-derived factor-1 secreted from stromal fibroblasts is a factor involved in invasion of cholangiocarcinoma. *Pathol Int* **56**, 381-389.
9. Alvaro, D. (2009) Serum and bile biomarkers for cholangiocarcinoma. *Curr Opin Gastroenterol* **25**, 279-284.
10. Farina, A., Dumonceau, J. M., and Lescuyer, P. (2009) Proteomic analysis of human bile and potential applications for cancer diagnosis. *Expert Rev Proteomics* **6**, 285-301.

11. Nishino, R., Honda, M., Yamashita, T., Takatori, H., Minato, H., Zen, Y., Sasaki, M., Takamura, H., Horimoto, K., Ohta, T., Nakanuma, Y., and Kaneko, S. (2008) Identification of novel candidate tumour marker genes for intrahepatic cholangiocarcinoma. *J Hepatol* **49**, 207-216.
12. Wang, A. G., Yoon, S. Y., Oh, J. H., Jeon, Y. J., Kim, M., Kim, J. M., Byun, S. S., Yang, J. O., Kim, J. H., Kim, D. G., Yeom, Y. I., Yoo, H. S., Kim, Y. S., and Kim, N. S. (2006) Identification of intrahepatic cholangiocarcinoma related genes by comparison with normal liver tissues using expressed sequence tags. *Biochem Biophys Res Commun* **345**, 1022-1032.
13. Tietz, P., de Groen, P. C., Anderson, N. L., Sims, C., Esquer-Blasco, R., Meheus, L., Raymackers, J., Dauwe, M., and LaRusso, N. F. (1998) Cholangiocyte-specific rat liver proteins identified by establishment of a two-dimensional gel protein database. *Electrophoresis* **19**, 3207-3212.
14. Grutzmann, R., Pilarsky, C., Ammerpohl, O., Luttgies, J., Bohme, A., Sipos, B., Foerder, M., Alldinger, I., Jahnke, B., Schackert, H. K., Kalthoff, H., Kremer, B., Kloppel, G., and Saeger, H. D. (2004) Gene expression profiling of microdissected pancreatic ductal carcinomas using high-density DNA microarrays. *Neoplasia* **6**, 611-622.
15. Luzzi, V., Mahadevappa, M., Raja, R., Warrington, J. A., and Watson, M. A. (2003) Accurate and reproducible gene expression profiles from laser capture microdissection, transcript amplification, and high density oligonucleotide microarray analysis. *J Mol Diagn* **5**, 9-14.
16. Sriuranpong, V., Mutirangura, A., Gillespie, J. W., Patel, V., Amornphimoltham, P., Molinolo, A. A., Kerekhanjanarong, V., Supanakorn, S., Supiyaphun, P., Rangaeng, S., Voravud, N., and Gutkind, J. S. (2004) Global gene expression profile of nasopharyngeal carcinoma by laser capture microdissection and complementary DNA microarrays. *Clin Cancer Res* **10**, 4944-4958.
17. Li, C., Hong, Y., Tan, Y. X., Zhou, H., Ai, J. H., Li, S. J., Zhang, L., Xia, Q. C., Wu, J. R., Wang, H. Y., and Zeng, R. (2004) Accurate qualitative and quantitative proteomic analysis of clinical hepatocellular carcinoma using laser capture microdissection coupled with isotope-coded affinity tag and two-dimensional liquid chromatography mass spectrometry. *Mol Cell Proteomics* **3**, 399-409.
18. Wang, Y., Rudnick, P. A., Evans, E. L., Li, J., Zhuang, Z., Devoe, D. L., Lee, C. S., and Balgley, B. M. (2005) Proteome analysis of microdissected tumor tissue using a capillary isoelectric focusing-based multidimensional separation platform coupled with ESI-tandem MS. *Anal Chem* **77**, 6549-6556.
19. Wulfkuhle, J. D., Sgroi, D. C., Krutzsch, H., McLean, K., McGarvey, K., Knowlton, M., Chen, S., Shu, H., Sahin, A., Kurek, R., Wallwiener, D., Merino, M. J., Petricoin, E. F., 3rd, Zhao, Y., and Steeg, P. S. (2002) Proteomics of human breast ductal carcinoma in situ. *Cancer Res* **62**, 6740-6749.
20. Pasa-Tolic, L., Lipton, M. S., Masselon, C. D., Anderson, G. A., Shen, Y., Tolic, N., and Smith, R. D. (2002) Gene expression profiling using advanced mass spectrometric approaches. *J Mass Spectrom* **37**, 1185-1198.
21. Shen, Y., Tolic, N., Masselon, C., Pasa-Tolic, L., Camp, D. G., 2nd, Lipton, M. S., Anderson, G. A., and Smith, R. D. (2004) Nanoscale proteomics. *Anal Bioanal Chem* **378**, 1037-1045.
22. Umar, A., Luider, T. M., Foekens, J. A., and Pasa-Tolic, L. (2007) NanoLC-FT-ICR MS improves proteome coverage attainable for approximately 3000 laser-microdissected breast carcinoma cells. *Proteomics* **7**, 323-329.
23. Dos Santos, A., Thiers, V., Sar, S., Derian, N., Bensalem, N., Yilmaz, F., Bralet, M. P., Ducot, B., Brechot, C., and Demaugre, F. (2007) Contribution of laser microdissection-based technology to proteomic analysis in hepatocellular carcinoma developing on cirrhosis. *Proteomics Clinical Applications* **1**, 545-554.

24. Wilm, M., Shevchenko, A., Houthaeve, T., Breit, S., Schweigerer, L., Fotsis, T., and Mann, M. (1996) Femtomole sequencing of proteins from polyacrylamide gels by nano-electrospray mass spectrometry. *Nature* **379**, 466-469.
25. Masselon, C. D., Kieffer-Jaquinod, S., Brugiere, S., Dupierris, V., and Garin, J. (2008) Influence of mass resolution on species matching in accurate mass and retention time (AMT) tag proteomics experiments. *Rapid Commun Mass Spectrom* **22**, 986-992.
26. Elias, J. E., and Gygi, S. P. (2007) Target-decoy search strategy for increased confidence in large-scale protein identifications by mass spectrometry. *Nat Methods* **4**, 207-214.
27. Dupierris, V., Masselon, C., Court, M., Kieffer-Jaquinod, S., and Bruley, C. (2009) A toolbox for validation of mass spectrometry peptides identification and generation of database: IRMa. *Bioinformatics* **25**, 1980-1981.
28. Monroe, M. E., Tolic, N., Jaitly, N., Shaw, J. L., Adkins, J. N., and Smith, R. D. (2007) VIPER: an advanced software package to support high-throughput LC-MS peptide identification. *Bioinformatics* **23**, 2021-2023.
29. Norbeck, A. D., Monroe, M. E., Adkins, J. N., Anderson, K. K., Daly, D. S., and Smith, R. D. (2005) The utility of accurate mass and LC elution time information in the analysis of complex proteomes. *J Am Soc Mass Spectrom* **16**, 1239-1249.
30. Fu, X., Gharib, S. A., Green, P. S., Aitken, M. L., Frazer, D. A., Park, D. R., Vaisar, T., and Heinecke, J. W. (2008) Spectral index for assessment of differential protein expression in shotgun proteomics. *J Proteome Res* **7**, 845-854.
31. Liu, H., Sadygov, R. G., and Yates, J. R., 3rd (2004) A model for random sampling and estimation of relative protein abundance in shotgun proteomics. *Anal Chem* **76**, 4193-4201.
32. Kearney, R. E., Blondeau, F., McPherson, P. S., Bell, A. W., Servant, F., Drapeau, M., de Grandpre, S., and Bergeron, J. J. M. (2005) Elimination of redundant protein identifications in high throughput proteomics. *2005 27th Annual International Conference of the IEEE Engineering in Medicine and Biology Society, Vols 1-7*, 4803-4806.
33. Prakash, A., Piening, B., Whiteaker, J., Zhang, H., Shaffer, S. A., Martin, D., Hohmann, L., Cooke, K., Olson, J. M., Hansen, S., Flory, M. R., Lee, H., Watts, J., Goodlett, D. R., Aebersold, R., Paulovich, A., and Schwikowski, B. (2007) Assessing bias in experiment design for large scale mass spectrometry-based quantitative proteomics. *Mol Cell Proteomics* **6**, 1741-1748.
34. Becker, R., Lenter, M. C., Vollkommer, T., Boos, A. M., Pfaff, D., Augustin, H. G., and Christian, S. (2008) Tumor stroma marker endosialin (Tem1) is a binding partner of metastasis-related protein Mac-2 BP/90K. *Faseb J* **22**, 3059-3067.
35. Koopmann, J., Thuluvath, P. J., Zahurak, M. L., Kristiansen, T. Z., Pandey, A., Schulick, R., Argani, P., Hidalgo, M., Iacobelli, S., Goggins, M., and Maitra, A. (2004) Mac-2-binding protein is a diagnostic marker for biliary tract carcinoma. *Cancer* **101**, 1609-1615.
36. Schmidt, V. A., Chiariello, C. S., Capilla, E., Miller, F., and Bahou, W. F. (2008) Development of hepatocellular carcinoma in Iqgap2-deficient mice is IQGAP1 dependent. *Mol Cell Biol* **28**, 1489-1502.
37. White, C. D., Brown, M. D., and Sacks, D. B. (2009) IQGAPs in cancer: a family of scaffold proteins underlying tumorigenesis. *FEBS Lett* **583**, 1817-1824.
38. Furubo, S., Harada, K., Shimonishi, T., Katayanagi, K., Tsui, W., and Nakanuma, Y. (1999) Protein expression and genetic alterations of p53 and ras in intrahepatic cholangiocarcinoma. *Histopathology* **35**, 230-240.
39. Momoi, H., Okabe, H., Kamikawa, T., Satoh, S., Ikai, I., Yamamoto, M., Nakagawara, A., Shimahara, Y., Yamaoka, Y., and Fukumoto, M. (2001) Comprehensive allelotyping of human intrahepatic cholangiocarcinoma. *Clin Cancer Res* **7**, 2648-2655.
40. Ohashi, K., Nakajima, Y., Kanehiro, H., Tsutsumi, M., Taki, J., Aomatsu, Y., Yoshimura, A., Ko, S., Kin, T., Yagura, K., and et al. (1995) Ki-ras mutations and p53 protein expressions in

intrahepatic cholangiocarcinomas: relation to gross tumor morphology. *Gastroenterology* **109**, 1612-1617.

41. Junking, M., Wongkham, C., Sripa, B., Sawanyawisuth, K., Araki, N., and Wongkham, S. (2008) Decreased expression of galectin-3 is associated with metastatic potential of liver fluke-associated cholangiocarcinoma. *Eur J Cancer* **44**, 619-626.
42. Schmitz, K. J., Lang, H., Wohlschlaeger, J., Sotiropoulos, G. C., Reis, H., Schmid, K. W., and Baba, H. A. (2007) AKT and ERK1/2 signaling in intrahepatic cholangiocarcinoma. *World J Gastroenterol* **13**, 6470-6477.
43. Kawase, H., Fujii, K., Miyamoto, M., Kubota, K. C., Hirano, S., Kondo, S., and Inagaki, F. (2009) Differential LC-MS-based proteomics of surgical human cholangiocarcinoma tissues. *J Proteome Res* **8**, 4092-4103.
44. Mikuriya, K., Kuramitsu, Y., Ryozaawa, S., Fujimoto, M., Mori, S., Oka, M., Hamano, K., Okita, K., Sakaida, I., and Nakamura, K. (2007) Expression of glycolytic enzymes is increased in pancreatic cancerous tissues as evidenced by proteomic profiling by two-dimensional electrophoresis and liquid chromatography-mass spectrometry/mass spectrometry. *Int J Oncol* **30**, 849-855.
45. Unwin, R. D., Craven, R. A., Harnden, P., Hanrahan, S., Totty, N., Knowles, M., Eardley, I., Selby, P. J., and Banks, R. E. (2003) Proteomic changes in renal cancer and co-ordinate demonstration of both the glycolytic and mitochondrial aspects of the Warburg effect. *Proteomics* **3**, 1620-1632.
46. Warburg, O. (1956) On the origin of cancer cells. *Science* **123**, 309-314.
47. Christofk, H. R., Vander Heiden, M. G., Harris, M. H., Ramanathan, A., Gerszten, R. E., Wei, R., Fleming, M. D., Schreiber, S. L., and Cantley, L. C. (2008) The M2 splice isoform of pyruvate kinase is important for cancer metabolism and tumour growth. *Nature* **452**, 230-233.
48. Liu, Y., Chen, Q., and Zhang, J. T. (2004) Tumor suppressor gene 14-3-3sigma is down-regulated whereas the proto-oncogene translation elongation factor 1delta is up-regulated in non-small cell lung cancers as identified by proteomic profiling. *J Proteome Res* **3**, 728-735.
49. Thomas, P. A., Kirschmann, D. A., Cerhan, J. R., Folberg, R., Seftor, E. A., Sellers, T. A., and Hendrix, M. J. (1999) Association between keratin and vimentin expression, malignant phenotype, and survival in postmenopausal breast cancer patients. *Clin Cancer Res* **5**, 2698-2703.
50. Wei, J., Xu, G., Wu, M., Zhang, Y., Li, Q., Liu, P., Zhu, T., Song, A., Zhao, L., Han, Z., Chen, G., Wang, S., Meng, L., Zhou, J., Lu, Y., Wang, S., and Ma, D. (2008) Overexpression of vimentin contributes to prostate cancer invasion and metastasis via src regulation. *Anticancer Res* **28**, 327-334.
51. Wu, M., Bai, X., Xu, G., Wei, J., Zhu, T., Zhang, Y., Li, Q., Liu, P., Song, A., Zhao, L., Gang, C., Han, Z., Wang, S., Zhou, J., Lu, Y., and Ma, D. (2007) Proteome analysis of human androgen-independent prostate cancer cell lines: variable metastatic potentials correlated with vimentin expression. *Proteomics* **7**, 1973-1983.
52. McInroy, L., and Maatta, A. (2007) Down-regulation of vimentin expression inhibits carcinoma cell migration and adhesion. *Biochem Biophys Res Commun* **360**, 109-114.
53. Jordan, M. A., and Wilson, L. (1998) Microtubules and actin filaments: dynamic targets for cancer chemotherapy. *Curr Opin Cell Biol* **10**, 123-130.
54. Pawlak, G., and Helfman, D. M. (2001) Cytoskeletal changes in cell transformation and tumorigenesis. *Curr Opin Genet Dev* **11**, 41-47.
55. Hall, A. (2009) The cytoskeleton and cancer. *Cancer Metastasis Rev* **28**, 5-14.
56. Yamaguchi, H., and Condeelis, J. (2007) Regulation of the actin cytoskeleton in cancer cell migration and invasion. *Biochim Biophys Acta* **1773**, 642-652.
57. Yan, B., Yap, C. T., Wang, S., Lee, C. K., Koh, S., Omar, M. F., Salto-Tellez, M., and Kumarasinghe, M. P. (2008) Cofilin immunolabelling correlates with depth of invasion in gastrointestinal endocrine cell tumors. *Acta Histochem.*

58. Janke, J., Schluter, K., Jandrig, B., Theile, M., Kolble, K., Arnold, W., Grinstein, E., Schwartz, A., Estevez-Schwarz, L., Schlag, P. M., Jockusch, B. M., and Scherneck, S. (2000) Suppression of tumorigenicity in breast cancer cells by the microfilament protein profilin 1. *J Exp Med* **191**, 1675-1686.
59. Shields, J. M., Rogers-Graham, K., and Der, C. J. (2002) Loss of transgelin in breast and colon tumors and in RIE-1 cells by Ras deregulation of gene expression through Raf-independent pathways. *J Biol Chem* **277**, 9790-9799.
60. Assinder, S. J., Stanton, J. A., and Prasad, P. D. (2009) Transgelin: an actin-binding protein and tumour suppressor. *Int J Biochem Cell Biol* **41**, 482-486.
61. Wittenmayer, N., Jandrig, B., Rothkegel, M., Schluter, K., Arnold, W., Haensch, W., Scherneck, S., and Jockusch, B. M. (2004) Tumor suppressor activity of profilin requires a functional actin binding site. *Mol Biol Cell* **15**, 1600-1608.
62. Heizmann, C. W., Fritz, G., and Schafer, B. W. (2002) S100 proteins: structure, functions and pathology. *Front Biosci* **7**, d1356-1368.
63. Schafer, B. W., and Heizmann, C. W. (1996) The S100 family of EF-hand calcium-binding proteins: functions and pathology. *Trends Biochem Sci* **21**, 134-140.
64. Chen, J. H., Ni, R. Z., Xiao, M. B., Guo, J. G., and Zhou, J. W. (2009) Comparative proteomic analysis of differentially expressed proteins in human pancreatic cancer tissue. *Hepatobiliary Pancreat Dis Int* **8**, 193-200.
65. Melle, C., Ernst, G., Schimmel, B., Bleul, A., Mothes, H., Kaufmann, R., Settmacher, U., and Von Eggeling, F. (2006) Different expression of calgizzarin (S100A11) in normal colonic epithelium, adenoma and colorectal carcinoma. *Int J Oncol* **28**, 195-200.
66. Wang, G., Wang, X., Wang, S., Song, H., Sun, H., Yuan, W., Cao, B., Bai, J., and Fu, S. (2008) Colorectal cancer progression correlates with upregulation of S100A11 expression in tumor tissues. *Int J Colorectal Dis* **23**, 675-682.
67. Stulik, J., Hernychova, L., Porkertova, S., Knizek, J., Macela, A., Bures, J., Jandik, P., Langridge, J. I., and Jungblut, P. R. (2001) Proteome study of colorectal carcinogenesis. *Electrophoresis* **22**, 3019-3025.
68. Orntoft, T. F., Thykjaer, T., Waldman, F. M., Wolf, H., and Celis, J. E. (2002) Genome-wide study of gene copy numbers, transcripts, and protein levels in pairs of non-invasive and invasive human transitional cell carcinomas. *Mol Cell Proteomics* **1**, 37-45.
69. Badea, L., Herlea, V., Dima, S. O., Dumitrascu, T., and Popescu, I. (2008) Combined gene expression analysis of whole-tissue and microdissected pancreatic ductal adenocarcinoma identifies genes specifically overexpressed in tumor epithelia. *Hepatogastroenterology* **55**, 2016-2027.
70. Mohammad, H. S., Kurokohchi, K., Yoneyama, H., Tokuda, M., Morishita, A., Jian, G., Shi, L., Murota, M., Tani, J., Kato, K., Miyoshi, H., Deguchi, A., Himoto, T., Usuki, H., Wakabayashi, H., Izuishi, K., Suzuki, Y., Iwama, H., Deguchi, K., Uchida, N., Sabet, E. A., Arafa, U. A., Hassan, A. T., El-Sayed, A. A., and Masaki, T. (2008) Annexin A2 expression and phosphorylation are up-regulated in hepatocellular carcinoma. *Int J Oncol* **33**, 1157-1163.
71. Zimmermann, U., Woenckhaus, C., Pietschmann, S., Junker, H., Maile, S., Schultz, K., Protzel, C., and Giebel, J. (2004) Expression of annexin II in conventional renal cell carcinoma is correlated with Fuhrman grade and clinical outcome. *Virchows Arch* **445**, 368-374.
72. Pena-Alonso, E., Rodrigo, J. P., Parra, I. C., Pedrero, J. M., Meana, M. V., Nieto, C. S., Fresno, M. F., Morgan, R. O., and Fernandez, M. P. (2008) Annexin A2 localizes to the basal epithelial layer and is down-regulated in dysplasia and head and neck squamous cell carcinoma. *Cancer Lett* **263**, 89-98.
73. Liu, J. W., Shen, J. J., Tanzillo-Swartz, A., Bhatia, B., Maldonado, C. M., Person, M. D., Lau, S. S., and Tang, D. G. (2003) Annexin II expression is reduced or lost in prostate cancer cells and its re-expression inhibits prostate cancer cell migration. *Oncogene* **22**, 1475-1485.

74. Gillette, J. M., Chan, D. C., and Nielsen-Preiss, S. M. (2004) Annexin 2 expression is reduced in human osteosarcoma metastases. *J Cell Biochem* **92**, 820-832.
75. Rajasekaran, A. K., and Rajasekaran, S. A. (2003) Role of Na-K-ATPase in the assembly of tight junctions. *Am J Physiol Renal Physiol* **285**, F388-396.
76. Barwe, S. P., Anilkumar, G., Moon, S. Y., Zheng, Y., Whitelegge, J. P., Rajasekaran, S. A., and Rajasekaran, A. K. (2005) Novel role for Na,K-ATPase in phosphatidylinositol 3-kinase signaling and suppression of cell motility. *Mol Biol Cell* **16**, 1082-1094.
77. Fleming, T. P., Ghassemifar, M. R., and Sheth, B. (2000) Junctional complexes in the early mammalian embryo. *Semin Reprod Med* **18**, 185-193.
78. Klymkowsky, M. W., and Savagner, P. (2009) Epithelial-mesenchymal transition: a cancer researcher's conceptual friend and foe. *Am J Pathol* **174**, 1588-1593.
79. Zavadil, J., and Bottinger, E. P. (2005) TGF-beta and epithelial-to-mesenchymal transitions. *Oncogene* **24**, 5764-5774.
80. Levy, L., and Hill, C. S. (2006) Alterations in components of the TGF-beta superfamily signaling pathways in human cancer. *Cytokine Growth Factor Rev* **17**, 41-58.
81. Benckert, C., Jonas, S., Cramer, T., Von Marschall, Z., Schafer, G., Peters, M., Wagner, K., Radke, C., Wiedenmann, B., Neuhaus, P., Hocker, M., and Rosewicz, S. (2003) Transforming growth factor beta 1 stimulates vascular endothelial growth factor gene transcription in human cholangiocellular carcinoma cells. *Cancer Res* **63**, 1083-1092.
82. Zen, Y., Harada, K., Sasaki, M., Chen, T. C., Chen, M. F., Yeh, T. S., Jan, Y. Y., Huang, S. F., Nimura, Y., and Nakanuma, Y. (2005) Intrahepatic cholangiocarcinoma escapes from growth inhibitory effect of transforming growth factor-beta1 by overexpression of cyclin D1. *Lab Invest* **85**, 572-581.
83. Keshamouni, V. G., Jagtap, P., Michailidis, G., Strahler, J. R., Kuick, R., Reka, A. K., Papoulias, P., Krishnapuram, R., Srirangam, A., Standiford, T. J., Andrews, P. C., and Omenn, G. S. (2009) Temporal quantitative proteomics by iTRAQ 2D-LC-MS/MS and corresponding mRNA expression analysis identify post-transcriptional modulation of actin-cytoskeleton regulators during TGF-beta-Induced epithelial-mesenchymal transition. *J Proteome Res* **8**, 35-47.
84. Guedj, N., Zhan, Q., Perigny, M., Rautou, P. E., Degos, F., Belghiti, J., Farges, O., Bedossa, P., and Paradis, V. (2009) Comparative protein expression profiles of hilar and peripheral hepatic cholangiocarcinomas. *J Hepatol* **51**, 93-101.

Figures captions:

Figure 1: Study design: Cholangiocytes microdissected from control livers (TB to TF) and from intrahepatic cholangiocarcinomas (CA to CD) were pooled prior to sample fractionation and LC-MS/MS analysis to generate an AMT tag database (A). Individual samples were subsequently analyzed by LC-FTMS to determine differential alterations of their proteome (B).

Figure 2: Quantitative LC-FTMS data quality control. (A) Chaorder plot for the 27 acquisitions (3 for each sample) color coded by sample. (B) Pairwise correlation matrix of peptide abundances measured in each acquisition sorted by sample.

Figure 3: Distributions of abundance indexes (AbI) for the 1121 peptides detected in both populations for the original data (A) and for the permuted data (B). The permutation allowed an estimation of the variance of the AbI measure under the assumption that all samples were equivalent. The dashed lines in panel A delimit the 95% confidence interval ($-0.24 < \text{AbI} < 0.53$), equal to the median AbI (0,14) of the original data plus or minus 1.96 times the standard deviation (0,199) of the permuted data; region where no change in abundance between the two populations was observed.

Figure 4: Expression analysis of Vimentin, Carbonic anhydrase 2 (CAII) and Profilin-1 in intrahepatic cholangiocarcinoma. (A) Cell plot of log of peptides abundances in cancer and control samples. Outline colors correspond to: peptides returned as significant by the statistical analysis (blue), peptides shared with other protein groups (pink), peptides not returned as significant by the statistical analysis (yellow) and population-specific peptides (grey). (B) Immunodetection of Vimentin, CAII and profilin-1. Western blots carried out as described in Material and Methods, were performed using microdissected tumorous and non-tumorous cholangiocytes from subjects included in the study. (C) Immunohistochemical analysis of vimentin and CAII. Immunohistochemistry was performed as described in Experimental procedures. Data from a

representative experiment including the tumorous and non tumorous areas of the liver of the patient CA and a control liver TB. Vimentin is expressed in tumorous cholangiocytes from ICC (a) and negative in non-tumorous cholangiocytes of peripheral (b) and perihilar (c) bile ducts. Internal controls as vascular smooth muscle cells and inflammatory cells are positive. Conversely, CAII is negative in tumorous cholangiocytes from ICC (d) and expressed in non-tumorous cholangiocytes of peripheral (e) and perihilar (f) bile ducts.

Figure 5: Vimentin expression in liver lesions by immunohistochemical staining using Tissue-microArray. (A) Representative cores of perihilar bile duct (1), intrahepatic cholangiocarcinoma (2), hilar cholangiocarcinoma (3) and hepatocellular carcinoma (4). IHC staining was performed as described in Experimental Procedures. Vimentin is negative in normal cholangiocytes from perihilar bile duct whereas inflammatory cells stained as positive internal controls (1). Vimentin is diffusely positive in the tumorous cholangiocytes from ICC (2) and totally negative in the tumorous cholangiocytes from hilar cholangiocarcinoma (3) and tumorous hepatocytes from HCC (4) (B) Vimentin expression in 23 intrahepatic cholangiocarcinoma, 17 hilar cholangiocarcinoma, 18 hepatocellular carcinoma and 22 controls patients (7 perihilar areas from liver without ICC, 4 normal livers from amyloid neuropathy and 11 non-tumoral counterparts of ICC). Staining was considered as negative when less than 5% of the cells of interest were immunostained. a) * $p < 0.001$ (Two-tailed Fisher's exact text)

Tables captions:

Table 1: Clinicopathological characteristics of patients used in MS study. All ICC samples (CA to CD) were CK7 positive and CK20 negative. Before surgery, patients did not receive any treatment. Perihilar areas from non-biliary pathology (TB to TF) were used as control samples.

Table 2: Identification of deregulated proteins in tumorous cholangiocytes. List of proteins identified with at least two proteotypic peptides and at least one of them detected with $AbI > 0.53$ or $AbI < -0.24$.

Supporting information

Supplementary Table 1: Database search parameters used for peptides identification.

Supplementary Table 2: Clinicopathologic features and vimentin expression of patients included in the tissue microarray. Positive (+) or negative (-) staining only concern cholangiocytes staining in control liver samples, ICC and hilar cholangiocarcinoma and hepatocytes in HCC.

Supplementary Table 3: Protein groups identified in the AMT database and corresponding protein accessions.

Supplementary Table 4: datasets resulting from the averaging of replicate analyses for the 4 cancer patients and the 5 controls.

Supplementary Table 5: Proteins covered exclusively by population specific peptides.

Supplementary Table 6: List of all peptides in the AMT tag database, their sequence, molecular weight, modifications when applicable, the corresponding protein groups, and information on proteotypicity.

Supplementary Figure 1: Microdissection of tumorous cholangiocytes. H&E stained liver sections before (A and B) and after (C) the laser microdissection of cholangiocytes.

Supplementary Figure 2: Individual tandem mass spectra for single hits proteins.

Supplementary Figure 3: Subcellular location of proteins of AMT tag database using Ingenuity Pathway Analysis.

Supplementary Figure 4: Analysis of Vimentin expression by IHC of the 4 invasive papillary cholangiocarcinomas included in TMA. a, b, c and d correspond to case 1, 2, 3 and 4 respectively

Table 1: Clinical data of the subjects included in the mass spectrometry analysis.

	ID	Gender	Age	Liver lesion	Tumor size	Histological type
Tumors	CA	F	39	Intrahepatic cholangiocarcinoma	7cm	Glandular structure
	CB	F	62	Intrahepatic cholangiocarcinoma	6cm	Mixed architecture
	CC	M	77	Intrahepatic cholangiocarcinoma	12cm	Glandular structure
	CD	M	55	Intrahepatic cholangiocarcinoma	14cm	Compact architecture
Controls	TB	M	48	Cirrhosis	-	-
	TC	M	53	Cirrhosis	-	-
	TD	F	45	Sub-acute hepatitis	-	-
	TE	F	61	Cirrhosis	-	-
	TF	M	53	Hepatocellular carcinoma	-	-

Table 2: Identification of deregulated proteins in tumorous cholangiocytes

Accession number	Protein Name	Gene name	Fold change Cancer / Normal	Sequence coverage	Unique peptides / proteotypic peptides	Protein Score	Postulated Biological process ^a
Proteins having peptides detected with increased abundance in tumorous samples							
VIME_HUMAN	Vimentin	VIM	9.26	68.5%	39/34	2496	cell motion
LDHB_HUMAN	L-lactate dehydrogenase B chain	LDHB	7.72	37.4%	11/10	808	monocarboxylic acid metabolic process
Q5JP53_HUMAN	Tubulin beta polypeptide	TUBB	4.76	33.8%	16/3	1098	cell motion
Q1WM23_HUMAN	Nucleoside diphosphate kinase	NME1	3.66	32.6%	8/8	431	regulation of cell proliferation, metastatic process
LDHA_HUMAN	L-lactate dehydrogenase A chain	LDHA	3.45	34.0%	10/9	620	anaerobic glycolysis
S10AB_HUMAN	Protein S100-A11 (Calgizzarin)	S100A11	3.01	43.8%	5/5	293	signal transduction, regulation of cell proliferation
ALDOA_HUMAN	Fructose-bisphosphate aldolase A	ALDOA	2.28	31.0%	10/10	531	actin cytoskeleton organization, hexose metabolic process
KPYM_HUMAN	Pyruvate kinase M2	PKM2	2.17	45.2%	20/20	1410	hexose metabolic process
A8K220_HUMAN	Peptidyl-prolyl cis-trans isomerase (Cyclophilin)	PPIA	2.16	50.3%	11/11	811	protein folding
K1C18_HUMAN	Keratin, type I cytoskeletal 18	KRT18	2.12	64.9%	33/32	2571	cell morphogenesis
PROF1_HUMAN	Profilin-1	PFN1	1.97	55.0%	8/8	457	actin cytoskeleton organization
Q6FG11_HUMAN	Transgelin-2	TAGLN2	1.86	33.2%	6/6	355	actin cytoskeleton regulation
PTMA_HUMAN	Prothymosin alpha	PTMA	1.86	21.6%	2/2	126	transcription
COF1_HUMAN	Cofilin-1	CFL1	1.70	50.0%	6/6	433	actin cytoskeleton organization
MDHC_HUMAN	Malate dehydrogenase, cytoplasmic	MDH1	1.68	29.9%	8/8	517	carboxylic acid metabolic process
HS90B_HUMAN	Heat shock protein HSP 90-beta	HSP90AB1	1.47	15.5%	11/5	739	molecular chaperone, protein folding
Proteins having peptides detected with decreased abundance in tumorous samples							
AGR2_HUMAN	Anterior gradient protein 2	AGR2	0.09	22.3%	4/4	208	unknown
CAH2_HUMAN	Carbonic anhydrase 2	CA2	0.09	25.4%	6/6	353	response to osmotic stress
ANX13_HUMAN	Annexin A13	ANXA13	0.23	33.9%	9/9	480	cell differentiation
A8K008_HUMAN	cDNA FLJ78387	-	0.26	11.2%	4/4	237	unknown
A0A5C9_HUMAN	IGLV2-14 protein	IGLV2-14	0.31	12.4%	2/2	107	unknown
K1C19_HUMAN	Keratin, type I cytoskeletal 19	KRT19	0.32	59.3%	32/21	2330	actin cytoskeleton organization
EST1_HUMAN	Liver carboxylesterase 1	CES1	0.32	34.0%	16/16	1091	metabolic process
LEG4_HUMAN	Galectin-4	LGALS4	0.35	12.7%	3/3	187	cell adhesion
HBA_HUMAN	Hemoglobin subunit alpha	HBA1	0.39	39.4%	6/6	328	oxygen transport
Q06AH7_HUMAN	Transferrin	TF	0.45	5.7%	4/4	172	iron ion transport
AT1A1_HUMAN	Sodium/potassium-transporting ATPase subunit alpha-1	ATP1A1	0.49	25.1%	19/19	1244	cellular ion homeostasis, carcinoma cell motility
ANXA4_HUMAN	Annexin A4	ANXA4	0.49	56.4%	23/23	1885	signal transduction, anti-apoptosis
ERLN2_HUMAN	Erlin-2	ERLN2	0.50	10.6%	3/3	180	unknown
ALBU_HUMAN	Serum albumin	ALB	0.51	56.5%	39/39	2418	transport
A4GX73_HUMAN	Hemoglobin subunit beta	HBB	0.51	75.5%	9/4	678	oxygen transport
A4D1PA_HUMAN	Aldo-keto reductase family 1, member B10	AKR1B10	0.55	13.6%	4/4	271	cellular lipid metabolic process
TALDO_HUMAN	Transaldolase	TALDO1	0.56	14.8%	5/5	213	carbohydrate metabolic process
A0A5E5_HUMAN	IGKC Protein	IGKC	0.57	24.2%	4/4	304	immune response
AK1C1_HUMAN	Aldo-keto reductase family 1 member C1	AKR1C1	0.62	14.6%	3/3	116	steroid metabolic process
HSP71_HUMAN	Heat shock 70 kDa protein 1	HSPA1A	0.63	27.5%	15/4	975	ubiquitin proteasome pathway, protein folding
PDIA3_HUMAN	Protein disulfide-isomerase A3	PDIA3	0.68	26.3%	11/11	646	protein folding
ANXA2_HUMAN	Annexin A2	ANXA2	0.79	53.1%	17/17	1189	actin cytoskeleton organization
A1A5C4_HUMAN	RRBP1 protein	RRBP1	0.80	10.6%	9/9	427	translation

a) Postulated biological process was determined by Gene Ontology (GO) and bibliographic features

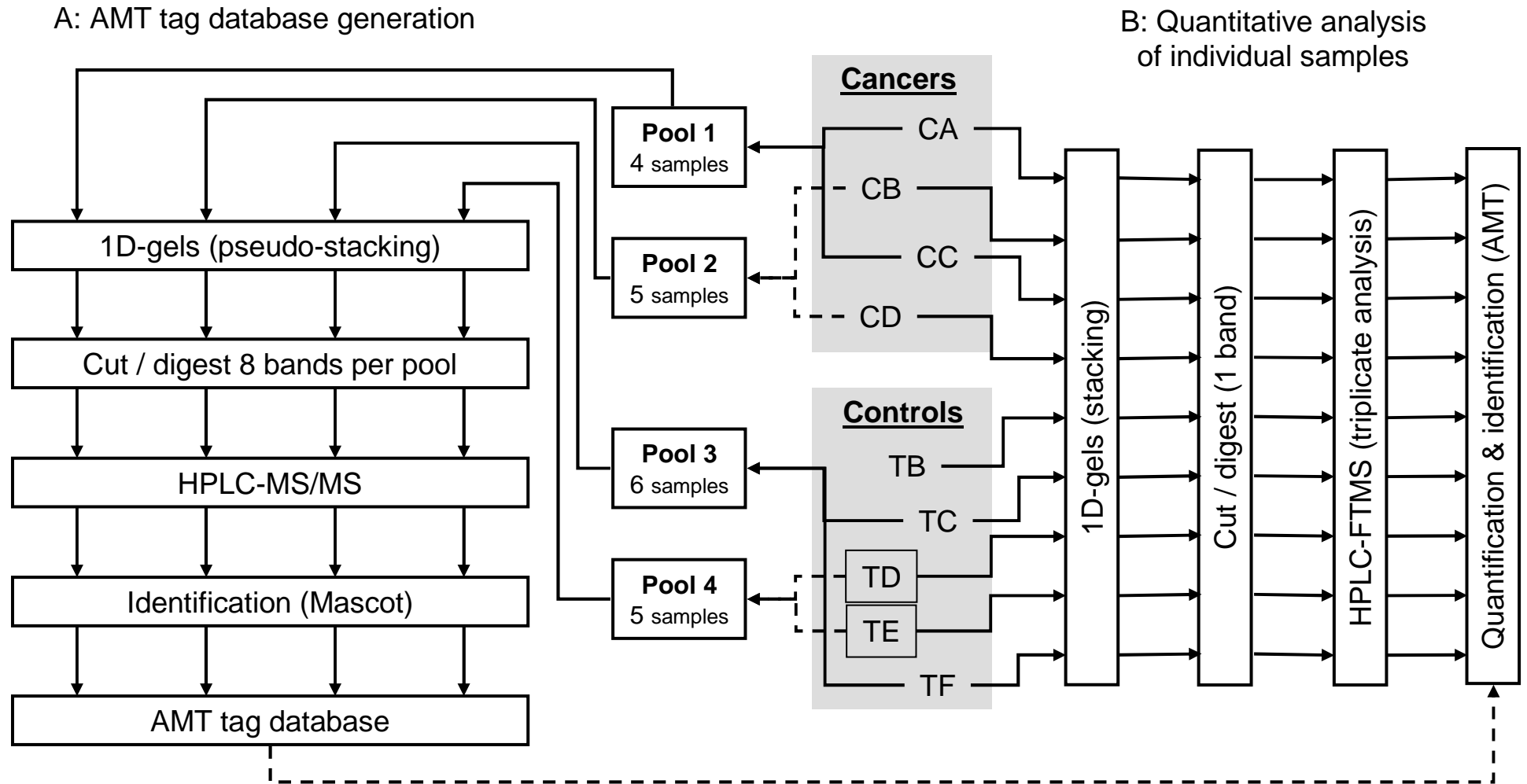


FIGURE 1

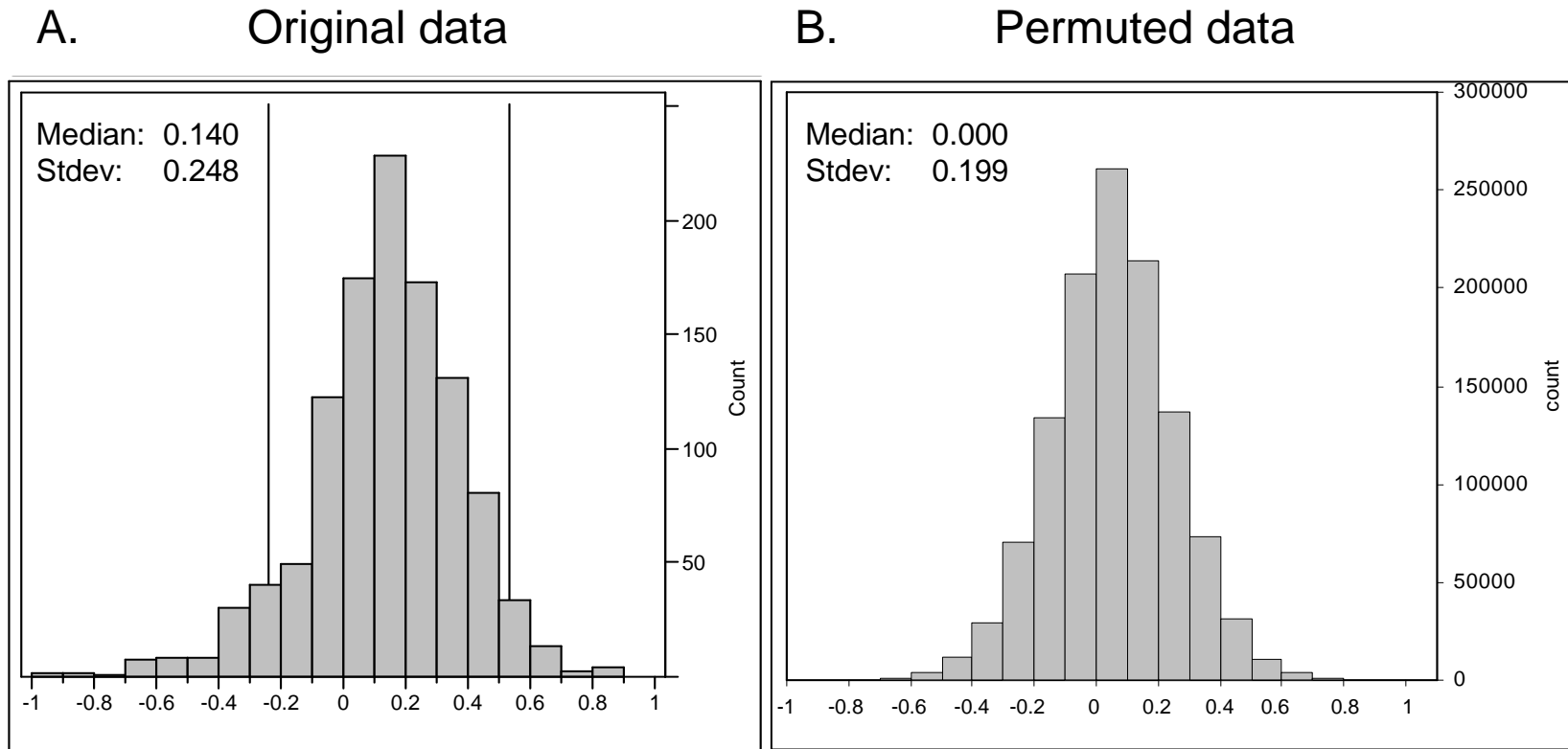
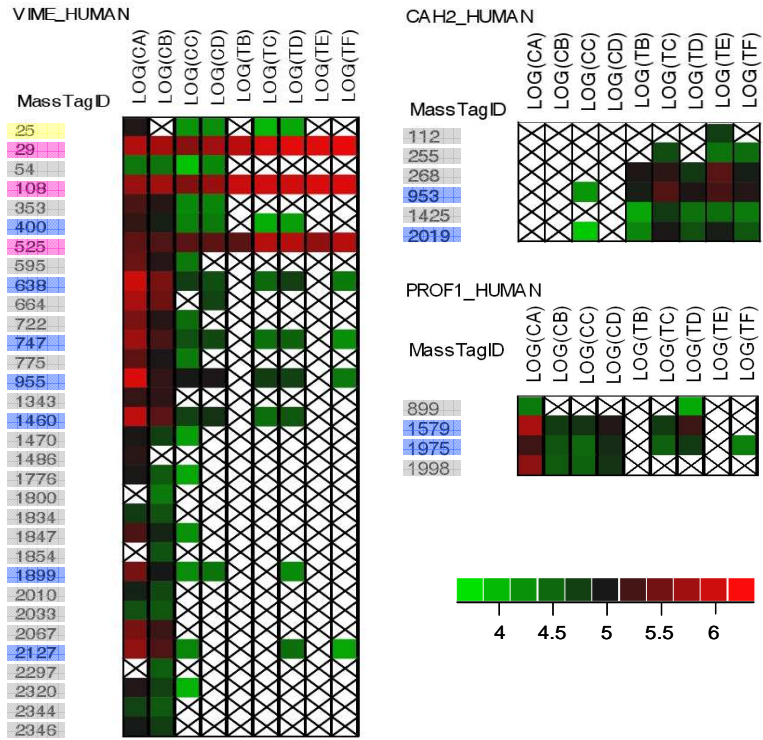
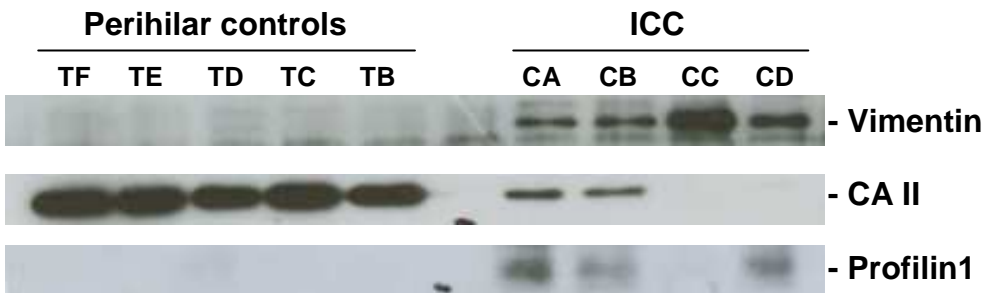


FIGURE 3

A



B



C

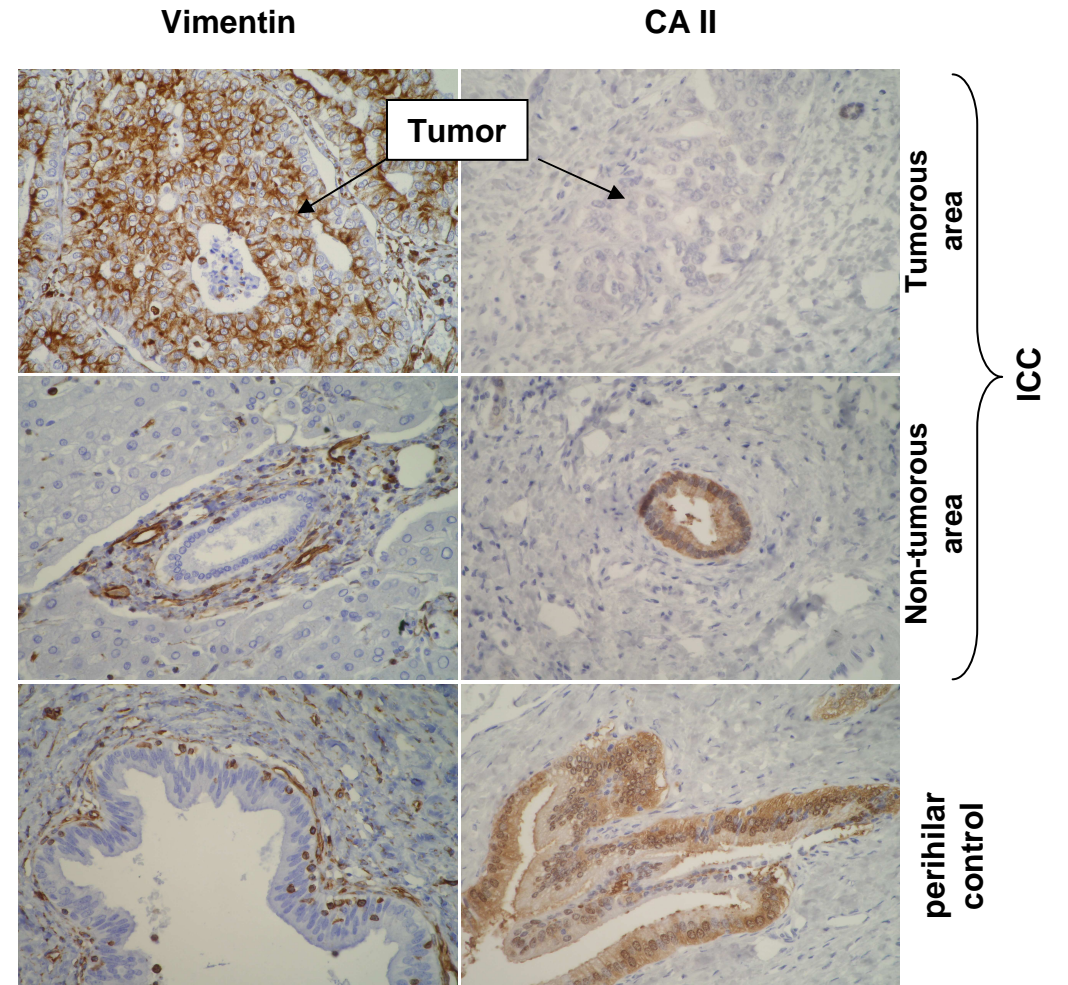
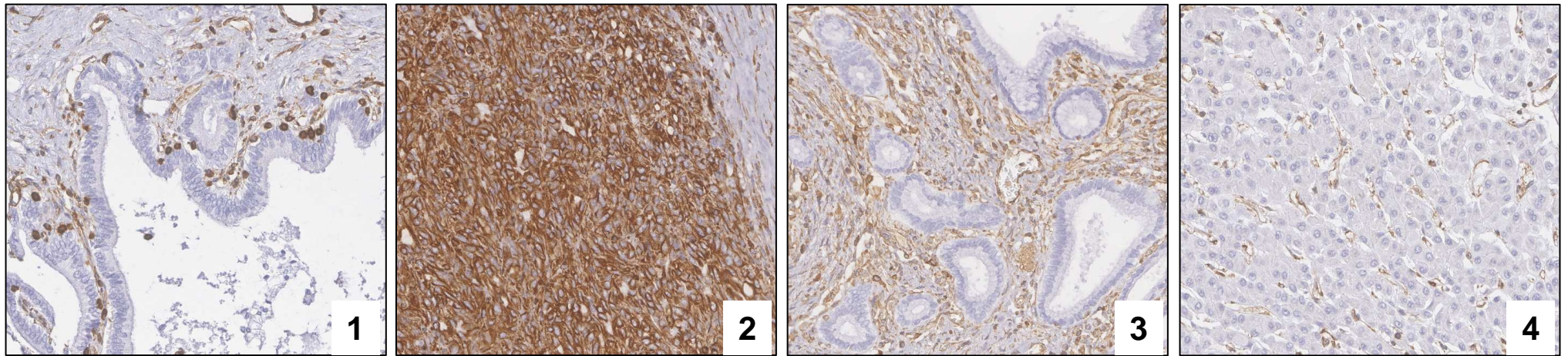


FIGURE 4

A



B

Tissue	Negative staining	Positive staining
Control samples	22	0
Intrahepatic cholangiocarcinoma	7	16
Hilar cholangiocarcinoma	15	2
Hepatocellular carcinoma	17	1

Statistical significance is indicated by asterisks (*). A bracket groups the positive staining counts for Intrahepatic cholangiocarcinoma (16) and Control samples (0), with an asterisk indicating significance. Another bracket groups the positive staining counts for Hilar cholangiocarcinoma (2) and Hepatocellular carcinoma (1), with an asterisk indicating significance. A third bracket groups the positive staining counts for Intrahepatic cholangiocarcinoma (16), Hilar cholangiocarcinoma (2), and Hepatocellular carcinoma (1), with an asterisk indicating significance.

FIGURE 5